

# 1 Introduction

Currently research, development, and production of technologies based on nanomaterials have leapt from its infancy several decades ago to high levels of commercial activities [1,2]. While much effort is on developing new technologies, most emphasis is on the improvement and consolidation of existing technologies based on initial potentials observed in nanosized materials. The growth and development in nanotechnology has been fundamentally propelled by inter-disciplinary cooperation in the areas of natural science, engineering, and business management. This cooperation facilitates speedy realization of ideas, as well as goal-oriented research based on a balanced economic strategy. The result is increasing financial and resource investment in nanotechnology, which is expected to exceed a \$1trillion by 2015 [3].

Nanoparticles, which are commonly defined as particles below 100 nm are considered the fundamental building blocks of most nanomaterial based devices. Many materials in nature (bulk) that exhibit special properties like magnetism, hardness, and different pigmentation, have fuelled the research towards the development of special devices and applications based on these properties. The properties of Nanomaterials differ from bulk due to higher atom concentration on the nanomaterial surface, with decreasing particle diameter. Hence, increased surface area to volume ratio is common for nanosized materials, in comparison to bulk [4]. Research interest in nanomaterials ranges from single elements like silicon and iron, through to nitrides, carbides and metal oxides ( $MO_x$ ), which is the focus of this research.

Metal oxides ( $MO_x$ ) occur naturally in different configuration, and have been exploited for millions of years due to their unique properties such as hardness, colour, porosity, brittleness etc. Zinc oxides ( $ZnO$ ), iron oxide ( $Fe_2O_3$ ), silicon oxide ( $SiO_2$ ) are some metal oxides that have sustainably been produced commercially in several million tons annually for several decades. The oxides have been engineered for applications in UV shielding cream, pigments, and catalysis. However, current investigations of these materials are revealing further properties, especially when these materials are processed (i.e. turned into transparent thin films) or “functionalized” (i.e. modification of the surface group). This has fuelled utilization of these materials for devices such as touch screen displays, gas sensors and solar cells.

The unique properties exhibited by metal oxides are due to their physico-chemical properties based on their particle size, morphology, crystallinity etc. Metal oxides can be electrically conducting, non-conducting or semi-conducting depending on their physical properties. Semi-conducting metal oxide particles are of particular interest because of the ease to influence their conductivity by varying parameters such as the ambient gas composition, particle size, temperature of exposure etc [5]. Nanosized tin oxide has been established as a semi-conducting metal oxide, which changes its conductivity under different conditions (oxidizing and reducing). This special feature of tin oxide makes it a potential material for gas-sensing, and is currently used in many solid state gas-sensing devices. However, its “response and relaxation time” (the time it takes to reach its maximum conductivity when exposed to a gaseous medium, and vice versa) is relatively low. Furthermore, tin oxide exhibits poor “sensitivity” (change of conductivity in the presence of a gaseous medium) towards some gases, which limits its applicability as a material for sensing diverse gases.

Titania ( $\text{TiO}_2$ ) is the most widely researched metal oxide, which is used for pigments and photo-mineralization of volatile organic compounds (*VOCs*). The photo-mineralization of  $\text{TiO}_2$  coupled with its transparency, makes it a widely used material for coating glass, which is sold as “self cleaning glass” by firms like Pilkington and Saint Gobain. However, this ability to reduce *VOCs* upon irradiation with light (UV) is constrained by low efficiency, due to the relatively low UV content of sunlight [6,7]. Research into nanosized  $\text{TiO}_2$  has revealed that doping titania with  $\text{Fe}_2\text{O}_3$  or nitrogen, results in a shift of the absorption spectrum of titania towards higher efficiency, upon exposure to sunlight. However, the transparency of the material is lost by this “functionalization” (material colour changes to red-brown due to  $\text{Fe}_2\text{O}_3$  content), hence the material cannot be used to coat transparent surfaces. Furthermore, the surface group of titania can be modified to make it hydrophilic or hydrophobic, whereby hydrophilicity of titania is essential for applications such as self cleaning glass.

These two illustrations of the applicability of nanosized  $\text{SnO}_2$  and  $\text{TiO}_2$  particles, establish the challenges posed by nanomaterials and the need for continued research into the factors that influence material properties. The synthesis route employed in generating semi-conducting  $\text{MO}_x$  nanoparticles significantly affects their properties (i.e. particle size, morphology and crystallinity). For most synthesis route, varying the experimental parameters directly influences the properties of the generated metal oxide

particles. Therefore, investigating the extent of these effects on the material, often serves as the basis for most synthesis based research on nanoparticles.

Several methods have successfully been employed for both laboratory and industrial synthesis of nanosized metal oxides [8-10]. The choice of synthesis route is often guided by the product, cost, safety etc. One such method is gas-phase synthesis of metal oxides in a flame reactor[11]. The advantages of this process include; wide operational scale (laboratory, pilot plant and industrial plants are possible), low operational cost, purity of product material, easy control of material properties by varying synthesis parameters and high product yield. For this synthesis route, the temperature-time history has been identified as one of the most important factors that influence particle size, crystallinity, and morphology [11]. A typical size dependent effect observed in  $MO_x$  was reported for premixed flame synthesized  $Fe_2O_3$  nanoparticles, whereby the blocking temperature of the particles were observed to vary between 50 and 150 K for particle diameters between 4 and 10 nm [12].

Several metal oxides ( $TiO_2$ ,  $GeO_2$ ,  $SnO_2$ ,  $SiO_2-Fe_2O_3$ ) have been successfully synthesized using different kinds of flame reactors [13-17]. However, for the purpose of this research a premixed  $H_2/O_2/Ar$  flame operated in a low-pressure reactor was used to synthesize a variety of single metal oxides and mixed oxide particles. The objective of this research is focused on the investigation into the synthesis of semi-conducting  $MO_x$  nanoparticles for well defined applications. Good theoretical understanding of the objectives, coupled with advanced characterization techniques, are required to set-up a synthesis structure, which in the middle of a constant feedback loop is necessary for continuous improvement of the synthesized  $MO_x$  nanoparticles. The fundamental queries that drove this study are as follows:

- a) What is the relationship between the experimental parameters such as temperature, pressure, residence time etc, on the structure and properties of the semi-conducting  $MO_x$ ?
- b) How can the properties of semi-conducting  $MO_x$  be tuned or improved for application purposes?
- c) How can deposition of semi-conducting  $MO_x$  nanoparticles on surfaces for characterization or incorporation in devices be achieved?

- d) Which characterization methods can deliver detailed information on material systems?

The premixed flame was chosen as the synthesis route for all investigations in this study, because of the huge success achieved with this method for the generation of  $\text{MO}_x$  nanoparticles [18,19]. The reactor equipped with an *in-situ* particle mass spectrometer for particle size analysis, was modified for the synthesis of diverse semi-conducting  $\text{MO}_x$  nanoparticles. *Ex-situ* characterization of the flame synthesized materials was performed with X-ray diffractometry (*XRD*) for information on crystal structure and composition. Brunauer-Emmett-Teller (*BET*) adsorption isothermal was used for surface area characterization. High resolution transmission electron microscope (*HR-TEM*) was used for information on particle-size, morphology, and composition. Impedance spectroscopy (*IS*) was used for information on conductivity and charge carrier transport, while ultraviolet-visible spectroscopy (*UV-VIS*) was used to obtain information on the optical absorption spectrum of the material.

In this study, the theory behind flame synthesis of  $\text{MO}_x$  particles is presented in chapter 2 for purpose of clarity and basic understanding of this thesis. Chapters 3, deals with characterization methods, flame reactor set-up, and various equipment description. Detailed results obtained from synthesis of  $\text{SnO}_2$ ,  $\text{TiO}_2$ ,  $\text{SnO}_2/\text{TiO}_2$  and diagnostic work on soot particles with time resolved laser induced incandescence (*TiRe-LII*) are presented in chapter 4. The summary of this dissertation is presented in chapter 5, while chapters 6 and 7 are the references and the appendix respectively.

## 2 Theory

### 2.1 General flame phenomena

Flames can simply be described as self propagating subsonic reaction wave usually with a luminous zone and heat release [20]. The terms, “premixed” and “diffuse” are commonly used to describe the mixing nature of combustion gases before ignition. The laminar premixed flame that was used for this research is characterized by the flame thickness and laminar burning velocity ( $v_f$ ), which is defined as the propagation velocity of a reaction zone normal to its surface and relative to the unburned gas. These properties are consequently influenced by fuel type, equivalence ratio, pressure, and temperature. The laminar burning velocity is important because it is the factor that describes the flame shape and stability properties such as blow-off and flashback [21]. The fundamental laminar burning velocity  $v_f$  is correlated to the speed of fresh gas  $v_g$  and speed of flame propagation  $v_p$  according to the following equation.

$$v_f = v_p \pm v_g \quad (2.1)$$

For flame propagation in similar direction as the flow of fresh gas, the minus operation in equation 2.1 is valid, and vice versa for counter gas flow and flame propagation. The following conditions will arise for varying laminar burning velocity and fresh gas speed velocity:

$$\text{Stationary flame front} \quad v_f = v_g \quad (2.2)$$

$$\text{Flashback} \quad v_f > v_g \quad (2.3)$$

$$\text{Blow-off} \quad v_f < v_g \quad (2.4)$$

Premixed flames are either operated as freely-propagating or burner-stabilized, whereby burner-stabilized are typically one dimensional (flat disc shaped flame). In burner stabilized flames, the gaseous reactants enter the flame with a velocity equal to the flame propagation velocity. This is followed by combustion reactions that proceed rapidly through a thin flame front yielding products and intermediates. However, since the flame heats the products, the product density is less than the reactant density, hence,

to ensure flame continuity, the burned gas velocity must be higher than that of the unburned gas.

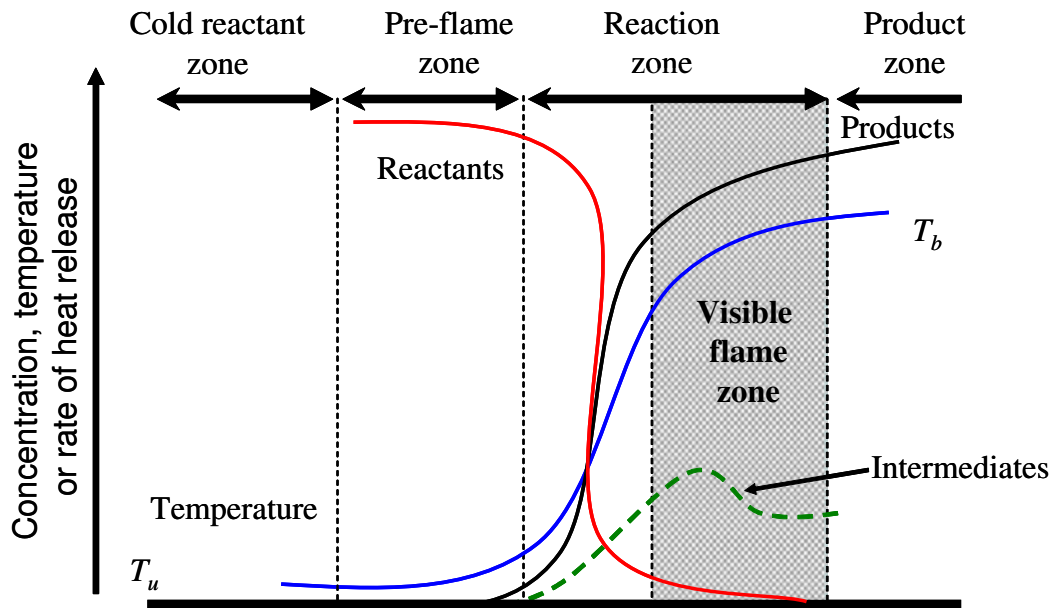


Figure 2.1: Profile of laminar flame showing temperature, reactants and products distribution [21]

Figure 2.1 shows temperature, reactants and products distribution across various zones of the laminar flame whereby  $T_u$  and  $T_b$  are the temperatures of the unburned gas and burned gas respectively. According to the detailed structure of the flame, the temperature increases smoothly from initial to final state, while the intermediates and products concentration will increase with decreasing reactant concentration. In the reaction zone the flame is often visible due to the luminescence of electronically excited species such as CH, CN,  $C_2$ , CHO and  $CO_2$ ; however, non-hydrocarbon systems such as  $H_2/O_2$  flames are invisible, whereby their presence can only be confirmed by measuring high temperatures radiating from the flame.

1-dimensional flat flame burners are often the burner of choice for combustion studies in laboratories and in some radiant burners. These burners can either be operated adiabatically, or non-adiabatically. For non-adiabatic flat flames, the burner head which is often a sintered matrix is water cooled. Constant extraction of heat from the flame via the water-cooled burner head decreases the laminar burning velocity, thereby allowing flames to be stabilized over a relatively wide range of flow conditions [22]. The ability to operate the flame under varying flow conditions is crucial for flame synthesis of materials, which often require varying inlet gas flow rates and compositions.

## 2.2 Parameters influencing premixed flame combustion synthesis

For the purpose of this research, premixed flame synthesis was selected as the route for the generation of nanosized semi-conducting  $\text{MO}_x$ . The premixed flame consists of hydrogen ( $\text{H}_2$ ) as fuel, oxygen ( $\text{O}_2$ ) as oxidizer and argon as inert gas component. The fuel/oxidant ratio, inert additives, pressure and temperature are the main factors that influence the laminar burning velocity and consequently the flame generated products.

### 2.2.1 Influence of fuel/oxidant ratio

The fuel/oxidant ratio is used for defining the upper (rich mixture) and lower (lean mixture) flammability limit, which establishes the region for sustainable combustion. When coupling flame chemistry with material synthesis (especially for  $\text{MO}_x$  generation), the fuel/oxidant ratio selected can influence the stoichiometry of the synthesized metal oxides [23,24].

The fuel/oxidant ratio also influences the flame temperature, whereby it is often assumed that a direct relationship exists between maximum flame temperature and maximum laminar burning velocity. However, this relationship varies with respect to different fuels and oxidants [25]. Maximum flame temperatures, as well as the overall temperature distribution during material synthesis, influence thermal dissociation of precursors, gas phase reaction of species, as well as sintering and surface growth phenomena of nanomaterials. The temperature-time profile during this process influences the properties, such as particle size, morphology and crystallinity of the material.

### 2.2.2 Influence of inert gas additives

The addition of inert gases such as argon (Ar), nitrogen ( $\text{N}_2$ ) and helium (He) to flames influences the physical properties of the flame such as temperature, conductivity and specific heat capacity, thermal diffusivity and chemical inhibitions of reactions [26]. For the synthesis of materials using varying concentration of Ar as an additive to the premixed  $\text{H}_2/\text{O}_2$  flame, significant changes in the physical properties of the particles are not expected. The inert gas additive serves as a “flexible” component of the inlet gas mixture, which can be varied to achieve a particular temperature or volumetric flow rate, so as to ensure flame stability. Furthermore, the cold gas inlet velocity can be

varied by changing the Ar content of the inlet gas mixture. This in turn can influence the residence time for particle growth in the reactor.

### **2.2.3 Influence of pressure**

The flammability limits of laminar premixed flames are also affected by a change in pressure. The limits for H<sub>2</sub> become slightly narrower with increasing pressure, while other hydrocarbons show the opposite effect with change in pressure[26]. During this research, operating the premixed flame under low-pressure conditions (typically at 30 mbar), was known to stretch the flame front. Information about the flame temperature and specie distribution within this extended front can thus be investigated with non-intrusive diagnostic methods. However, unlike the velocity of fresh gas that can be widely varied, the change in reactor pressure is limited to a small range (between 20 and 60 mbar), whereby operations outside this range can lead to either blow-off or a pulsating flame front. Increase in reactor pressure slightly increases the mean particle diameter of synthesized nanomaterials and in some cases the particle morphology [27].

### **2.2.4 Influence of temperature distribution**

The temperature distribution of the 1-dimensional premixed, burner-stabilized H<sub>2</sub>/O<sub>2</sub>/Ar flame, operated in low-pressure regimes, can be influenced by the cold gas flow, the gas mixing ratio and the inert gas content. Results from the temperature distribution has been simulated or measured with thermocouples and reported [28,29]. The obtained results often do not adequately compensate for the heat loss by radiation, which is sometimes difficult to incorporate into the measurement and analysis algorithm. The maximum flame-temperature and temperature-distribution are important for the thermal dissociation of the precursor during particle synthesis. Whereby, they influence the coagulation and coalescence steps of the particle formation process. Hence the mean particle diameter, particle size distribution and particle morphology are influenced by this factor. Furthermore, the temperature profile may determine if a doped, segregated or nanocomposite arrangement will be generated for the selected synthesis route.

## **2.3 Fundamentals of gas-to-particle conversion**

Low-pressure, gas-phase synthesized materials are often characterized by small particle size, narrow particle size distribution, and spherical morphology. The most important step during gas phase synthesis is the gas-to-particle conversion, which involves several

overlapping step rapidly occurring within a very short time frame. These steps are hereby presented for both single component  $\text{MO}_x$  and multi-component material system synthesis.

### 2.3.1 Gas-to-particle conversion for single component metal oxide ( $\text{MO}_x$ ) systems

Gas-to-particle conversion that yields a single component metal oxide ( $\text{MO}_x$ ) occurs by condensation of supersaturated species in the low-pressure flame reactor. Upon introduction into the flame, some dilute precursor vapour containing the metal source such as iron pentacarbonyl  $\text{Fe}(\text{CO})_5$  is thermally dissociated, followed by a gas-phase reaction with oxygen, nucleation, and condensation of particles at lower temperatures downstream of the flame (see Figure 2.2). Other precursors such as titanium tetraisopropoxide TTIP and tetraethoxysilane TEOS, do not require additional oxygen in order to generate the metal oxide, due to the sufficient oxygen content of the precursor. As the particle concentration increases due to condensation, the particle growth mechanism becomes more a function of coagulation, coalescence, and surface growth, which leads to a mix of agglomerated and non-agglomerated particles with varying particle diameter (see Figure 2.2).

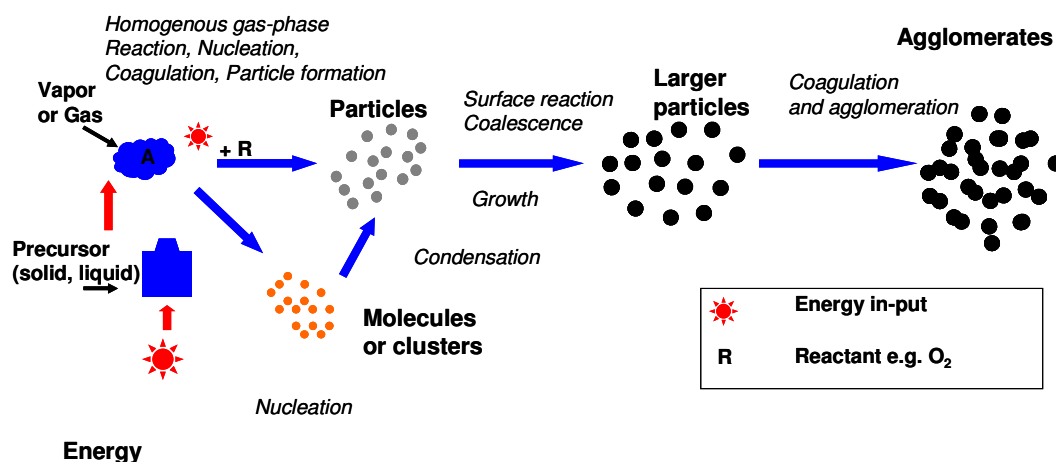


Figure 2.2: Gas-to-particle conversion for a single component powder generation [30]

Several models, theories and dissertations have been proposed to describe in detail the fluid and particle dynamics, transport, and chemical phenomena involved with gas-phase synthesis of particulate materials [31-33]. From all these methods, the *general dynamic equation (GDE)* is widely used to model gas-to-particle conversion [32]. It describes the aerosol dynamics with respect to the particle size distribution;

furthermore, it encompasses nucleation, condensation, coagulation and coalescence, and is expressed [34,35] as:

$$\frac{\partial n}{\partial t} + \frac{\partial(Gn)}{\partial v} - I_f(v^*)\delta(v-v^*) = \frac{1}{2} \int_0^v \beta(v-v',v')n(v-v',t)n(v',t)dv' - n(v,t) \int_0^\infty \beta(v,v')n(v',t)dv' \quad (2.5)$$

a
b
c

d
e

The property  $n$  is number concentration of the particles,  $v$  is particle volume,  $v^*$  is the critical volume,  $v'$  is the average particle volume,  $\beta$  is the collision frequency of the particles and  $t$  is time. The first term (a) in the equation describes the rate of change of the particle size distribution with time (particle concentration). The second term (b) involves the growth law, which represents the gain or loss of particles within a size range by condensation, while the third term (c) on the left hand side describes the formation of new particles with critical size  $v^*$  by nucleation at the rate of  $I_f$ . The other two terms (d and e), describe the gains and loss of particles within a given volume class as a result of Brownian coagulation. Equation 2.5 is however, only valid for spherical particles, and does not take into account particle diffusion as well as velocities due to external forces (e.g. thermophoresis).

### 2.3.1.1 Homogenous nucleation

Homogenous nucleation occurs when clusters grow to a size whereby the rate of formation is higher than the rate of destruction. This implies that homogeneously nucleated clusters are larger than the critical cluster size [36]. Nucleated clusters are sometimes thermodynamically unstable due to evaporation and partial pressure influences, unless they are sufficiently large enough, and partial pressure conditions around the cluster is greater than vapour pressure above the curved surface of the cluster (*Kelvin effect*) [30]. Thus, the highly supersaturated state necessary for nucleation is achieved by decreasing the equilibrium vapour pressure through cooling of the gas. In order for clusters to grow and form particles, the saturation ratio (which is the ratio of the actual pressure of the specie, to the equilibrium vapour pressure over a flat surface) must be above 1.